



ELSEVIER

Contents lists available at ScienceDirect

Deep-Sea Research II

journal homepage: www.elsevier.com/locate/dsr2

Controls of seasonal variability of phytoplankton blooms in the Pearl River Estuary

Zhongming Lu^{b,*}, Jianping Gan^{a,b}

^a Department of Mathematics, Hong Kong University of Science and Technology, Kowloon, Hong Kong, China

^b Division of Environment, Hong Kong University of Science and Technology, Kowloon, Hong Kong, China

ARTICLE INFO

Keywords:

Pearl River Estuary
Phytoplankton
Bloom
Chlorophyll
Seasonal variability
Residence time
Water column stability
Turbidity

ABSTRACT

Based on both physical and biological data collected from cruises in different seasons between 2010 and 2011, we found that the phytoplankton bloom was highly seasonally variable along the longitudinal axis of the Pearl River Estuary (PRE) and was confined to very limited locations because of the variation in the coupled physical–biological forcing of the phytoplankton growth and accumulation. We investigated the relative importance and joint control of the bloom's variation by freshwater residence time, water column stability, and light limitation that were governed by river discharge, vertical mixing, and turbidity in the PRE, respectively. We found that the bloom occurred in the middle of the well/partially mixed estuary during the dry season when river discharge was relatively small. Although the water nutrient concentration and residence time were favorable for phytoplankton accumulation during this season, the bloom was absent in the upper and lower parts of the estuary likely associated with high turbidity in the upper region and strong vertical mixing in the lower region. In contrast, strong river discharge during the wet season pushed the nutrient-rich river plume farther seaward and formed a salt-wedged estuary. With a stable water column and relatively low turbidity during this season, the bloom could only occur in the lower part of the estuary where the phytoplankton growth rate was greater than the water turnover rate.

© 2014 Elsevier Ltd. All rights reserved.

1. Introduction

An estuary is an important transition zone where river water and seawater meet and mix (Pritchard, 1967). Freshwater discharge and salt water intrusion form a unique estuarine hydrodynamic system and regulate the biogeochemical processes. The complex interactions between physical and biogeochemical factors within the estuarine ecosystem make it difficult to define the factors that regulate the growth and distribution of phytoplankton.

Nutrient limitation is often considered to be a major control of biological production. The phytoplankton bloom is often regulated by different nutrient species, mainly nitrogen, phosphorus, and silicon (e.g. Malone et al., 1996; Myers and Iverson, 1981; Twomey and Thompson, 2001; Yin et al., 2000). Light availability is another important factor that controls phytoplankton growth and distribution. Its importance is a result of high suspended particle loading, waste water discharge, and the turbidity maximum induced by physical and chemical processes. Generally, light is the major regulator of phytoplankton growth during winter, when water is turbid due to intensified vertical mixing, or during high runoff

(Mallin et al., 1999; Pennock and Sharp, 1994). Hydrodynamic conditions are also important factors for development of phytoplankton blooms in an estuary. Water residence time and water column stratification/stability are well-known to be necessary conditions for the formation of a bloom. Longer residence time is generally more likely to induce a phytoplankton bloom (Huzzey et al., 1990). The variation of water residence time in an estuary will lead to the shift of the bloom location (e.g. Lucas et al., 1999). The effect of water column stability on phytoplankton is more complex. Strong vertical stratification, for example, can effectively block the vertical mass and energy exchanges, and, as a result, confine the phytoplankton to a shallow surface layer with strong irradiance and isolate the phytoplankton from bottom grazers (Cloern, 1991, 1996; Koseff et al., 1993; Masson and Pena, 2009).

Estuaries are highly diverse physical–biological systems. Various factors that control phytoplankton bloom and the response to these factors are variable in different estuaries, at different locations within a given estuary, and at different times (Monbet, 1992). In the ocean, variability of the phytoplankton bloom is concurrently regulated by combined physical and biological controls. For example, when nutrients are limited in the surface layer, weak stability in the water column allows nutrient replenishing in the euphotic layer and makes a bloom possible (O'Boyle and Silke, 2010; Tremblay et al., 1997). Identification of all controlling factors

* Corresponding author.

E-mail address: luzm@ust.hk (Z. Lu).

and their combined effect is the key to rationalizing the formation of the bloom in an estuary that is forced by complex physical-biological processes.

The Pearl River Estuary (PRE) is a subtropical estuary embedded in the southern coast of China and connected with the continental shelf of the Northern South China Sea (NSCS, Fig. 1). It is triangular with Guangzhou at its northern apex, and Macau and Hong Kong at the southwest and southeast corners, respectively. The PRE has several very unique characteristics. It receives huge freshwater discharge with an annual average flow rate around $10,000 \text{ m}^3 \text{ s}^{-1}$ (Zhai et al., 2005). The Pearl River is the 13th largest river in the world and the 2nd largest river in China in terms of freshwater discharge. The estuary encompasses a large area of about 1900 km^2 and extends about 60 km from the river mouth to the open shelf. Its width varies from $\sim 10 \text{ km}$ in the upper reach to $\sim 60 \text{ km}$ in the lower reach and is wide enough that shelf circulation influences the lower estuary and not just the gravitational circulation as in a traditional estuarine hydrodynamics (Zu and Gan, this issue). The physical and biogeochemical processes in the PRE have strong seasonality because of the southwesterly/northeasterly monsoon in summer/winter and the significant seasonal variation of river discharge. About 80% of the discharge from the Pearl River happens during the wet season from April to September (Zhai et al., 2005). Meanwhile, variability induced by tidal forcing of $\sim 1 \text{ m}$ magnitude exerts additional high frequency variation on the seasonal processes.

Due to the fast development of industrial and agricultural activities and urbanization in the last 30 years, the PRE receives a very high load of anthropogenic nutrients. Dissolved Inorganic Nitrogen (DIN; NO_3^- , NO_2^- , NH_4^+) is the main component of the anthropogenic nutrient input, and the N/P ratio in the PRE is generally very high, ranging from ~ 30 in the lower estuary to over 100 in the upper estuary (Harrison et al., 2008; Huang et al., 2003; Zhang et al., 1999). This provides the potential for phosphate limitation (Xu, 2007). Meanwhile, the DIN and phosphate concentration is generally above $20 \mu\text{M}$ and $0.5 \mu\text{M}$ in most parts of the estuary, respectively. This is obviously higher than the half-saturation concentrations for phytoplankton uptake of DIN (generally $0.5\text{--}2 \mu\text{M}$) and phosphate

(generally $0.07\text{--}0.5 \mu\text{M}$) (Chen et al., 2002; Fennel et al., 2006; Guillaud et al., 2000; Liu and Yin, 2007; Parekh et al., 2005), which indicates that nutrients may not limit phytoplankton growth in the region.

Although the nutrient concentration in the PRE is high, the phytoplankton biomass is not as high as one would expect, and there is no frequently occurring large scale hypoxia (Yin et al., 2004). The effect of zooplankton grazing on chlorophyll or primary production is also relatively minor. Tan et al. (2004) found that the grazing impact for zooplankton on chlorophyll in the PRE is only about $20 \pm 21.5\%$ during the wet season and $4.5 \pm 3.2\%$ during the dry season. To explain this phenomenon, dilution of phytoplankton biomass due to river discharge, estuarine circulation, and vertical mixing due to wind and tidal effects were studied and proposed as potential regulating factors (Harrison et al., 2008; Yin and Harrison, 2007). Yet there is no systematic and comprehensive study on the seasonality of the phytoplankton bloom in the PRE. In particular, combined physical and biogeochemical field measurements on a seasonal time scale have not been documented. In addition, the qualitative description or multi-factor regressions that were used in previous studies may not be sufficient to identify the inherent controlling mechanisms for the temporal and spatial variations of phytoplankton biomass (Huang et al., 2004). A quantitative or quasi-quantitative analysis on the correlation between estuarine hydrodynamics and ecosystem response has never been provided for the PRE.

In this study, we used seasonal observations to quantify, for the first time, the relative importance of water residence time, water column stability, and turbidity on the formation of the phytoplankton bloom in the PRE. We explored the possibility of bloom occurrence under single/multiple regulator(s), and provided explanations for the temporal and spatial variation of the blooms that were observed.

2. Materials and methods

This study is a part of the PRE time-series observation project that was carried out from March 2010 to March 2011. Four cruises were conducted in 2010 from March 29 to April 2, from August 1 to 2, from November 7 to 8, and from December 27, 2010 to January 1, 2011. These represented typical spring, summer, autumn, and winter conditions, respectively. The field observations were carried out along sections A, B, L, and C (Fig. 1). Longitudinal section A was used to identify seasonal chlorophyll variation along the estuary. The spatial intervals of sampling were $\sim 7 \text{ km}$ along section A and $\sim 5 \text{ km}$ along the other sections. We conducted a supplementary cruise on 7 July 2011 to obtain the turbidity distribution along section A. The variation of the Pearl River discharge during this period was represented by data from the Xijiang River (a.k.a. West River, one of the most important tributaries of the Pearl River) (Fig. 2). Daily flow rate was obtained from the Information Center of Water Resources (Bureau of Hydrology, the Ministry of Water Resources of PR China) (<http://xxfb.hydroinfo.gov.cn/EN/index4winter.jsp>). The freshwater discharge received by the PRE can be estimated according to the discharge ratio between different outlets. For convenience, we separated the estuary into upper and lower estuaries using Inner Lingding Island as the dividing point.

In situ salinity, temperature, and chlorophyll were measured at a sampling rate of 8 Hz by a SBE-25 SEALOGGER CTD (Conductivity-Temperature-Depth) profiling system that was calibrated by the manufacturer just before the field survey (Sea Bird Electronics, Inc.). The accuracy of the CTD profiling system is $0.002 \text{ }^\circ\text{C}$, 0.0003 S/m , and 0.1% of full scale range for temperature, conductivity, and pressure, respectively, and the resolution is $0.0003 \text{ }^\circ\text{C}$, 0.00004 S/m , and 0.015%

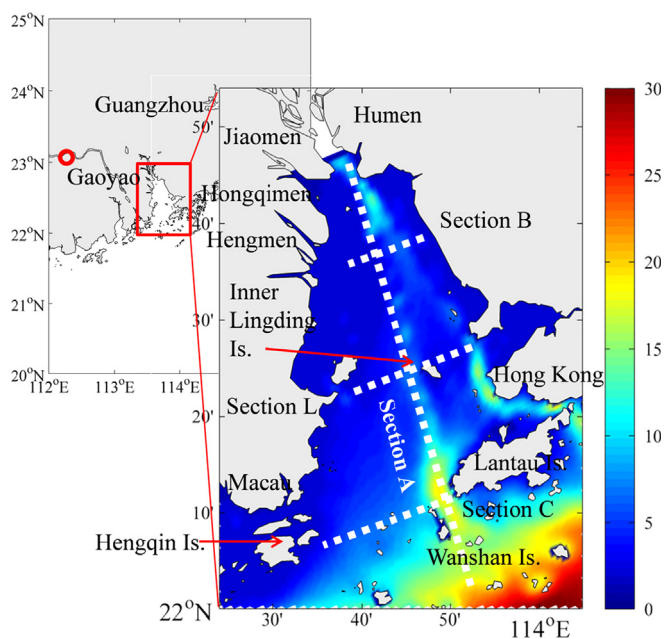


Fig. 1. Map of the Pearl River Estuary. The thick dashed lines are the survey sections and the color contours show the bathymetry (m). The red circle denotes the Gaoyao hydrological station. (For interpretation of the references to color in this figure caption, the reader is referred to the web version of this paper.)

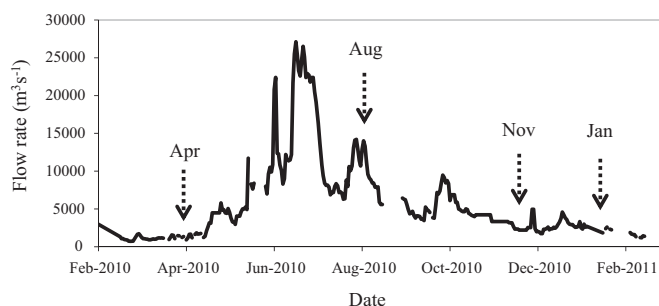


Fig. 2. The flow rate of the Xijiang River during the study period. River discharge data were obtained from Gaoyao hydrological station (Fig. 1).

Table 1

Cruise time and river flow rate. The flow rate of the upper four outlets = flow rate of Xijiang/68.5% × 53%.

Surveying time	Season	River flow rate ($\text{m}^3 \text{s}^{-1}$)	
		Xijiang	Upper four outlets*
March 29–April 2, 2010	Spring	1500	1161
August 1–2, 2010	Summer	14,000	10,832
November 7–8, 2010	Autumn	3300	2553
December 27, 2010–January 1, 2011	Winter	3100	2399

* The four outlets are Humen, Jiaomen, Hongqimen, and Hengmen.

of full scale range, respectively. The CTD profiling system was lowered and raised in the water column at a rate of $\sim 0.2 \text{ m/s}$. The current velocity was measured by a WHS-300 Workhorse Acoustic Doppler Current Profiler (ADCP) system (Teledyne RD Instruments) at a vertical resolution of 0.5 m with a working frequency of 300 kHz . Surface water turbidity (at $\sim 1 \text{ m}$ depth) was measured by an YSI 6600V2 Multiparameter Water Quality Sondes (YSI Incorporated). Water transparency (Secchi depth) was measured by a 30-cm diameter white Secchi disk.

3. Results

3.1. Seasonal hydrographic characteristics

The PRE is significantly affected by the seasonal variation of freshwater discharge from the Pearl River. During the four cruises of this study, the discharge rate of the Xijiang River varied with a range from $\sim 1500 \text{ m}^3 \text{ s}^{-1}$ in the dry season to $\sim 14,000 \text{ m}^3 \text{ s}^{-1}$ in the wet season (Fig. 2). The volume discharge rate received by the PRE (Table 1) can be derived by taking the Xijiang River as $\sim 68.5\%$ of the total Pearl River discharge and the combined runoff discharged into the estuary from the four outlets (Humen, Jiaomen, Hongqimen, and Hengmen) in the upper estuary as $\sim 53\%$ of the total Pearl River discharge (Zhai et al., 2005).

Hydrographic variability in the PRE is also distinctly seasonal as is shown by the vertical structures of salinity (Fig. 3) along section A. In the dry season, the water column was generally well-mixed (Fig. 3A, C, and D), especially in the lower part of the estuary due to the enhanced vertical motion at the plume front (Zu, 2009). The PRE was a partially or well-mixed estuary during the dry season and was a typical salt-wedge (Fig. 3B) estuary in the wet season. A front separated the upper fresh river water from seawater in the mid-estuary in the dry season and it became sharper near the entrance and tilted landward with depth in the wet season. Evidently, the magnitude of the river discharge (Fig. 2) characterized the seasonal water mass distributions in the PRE.

3.2. Spatial and seasonal variability of the phytoplankton bloom

Considering the complex hydrodynamic conditions in the PRE, we designed three additional cross-estuary sections (B, L, and C) in our field study, aside from section A, to see the horizontal distribution of different variables. Fig. 4 shows the horizontal distribution of density and chlorophyll during the dry and wet seasons. The horizontal distribution of density (Fig. 4A and B) shows that there is a significant north to south gradient and that the contours of constant density tilted southwestward in both dry and wet seasons. The high chlorophyll zone (Fig. 4C and D) was mainly confined to the mid-estuary for the dry season and to the lower estuary for the wet season, and did not reflect the strong physical regulation of the phytoplankton distribution. Obviously, the three cross-estuary sections did not sufficiently cover the potential bloom regions to resolve the horizontal distribution of chlorophyll and could not provide sufficient information for us to investigate its horizontal structure and control mechanisms. Therefore, in this study, we will focus on section A to investigate the spatial and seasonal variability of the phytoplankton bloom.

The nutrient distribution varied along the PRE, ranging from several μM in the lower estuary to over $100 \mu\text{M}$ in the upper estuary for $\text{NO}_3 + \text{NO}_2$, and from $\sim 0.5 \mu\text{M}$ in the lower estuary to over $1 \mu\text{M}$ in the upper estuary for PO_4 (Cai et al., 2004; Dai et al., 2008; He et al., 2010). Although the PRE's nutrient load is very high, we did not observe a persistent phytoplankton bloom over the entire estuary. The phytoplankton blooms were always confined to very limited locations during all four cruises as is shown by the vertical distributions of chlorophyll along section A (Fig. 5). Chlorophyll maxima occurred distinctly in particular places in the PRE during different seasons. In general, the blooms were generated in mid-estuary (between $\sim 22.4^\circ\text{N}$ and 22.5°N) in the dry season (Fig. 5A, C, and D), but moved to the lower reach of the estuary during the wet season (Fig. 5B).

By carefully examining the chlorophyll distribution for the different seasons, we found that there were different bloom patterns in the PRE. These differences occurred not only in wet and dry seasons, but also within the dry season itself. The bloom was strong and concentrated in the upper- and mid-estuary in spring (Fig. 5A), and mid-estuary in autumn (Fig. 5C). However, the bloom was relatively weak and spatially dispersed over the estuary and had a concurrent chlorophyll maximum in the mid-estuary (Fig. 5D) in winter. The high chlorophyll value in the upper reach during the spring cruise was likely induced by the inactive phytoplankton from the river discharge instead of by cells generated locally. This speculation is supported by the low level of dissolved oxygen measured at the same location (Fig. 6A) because high phytoplankton productivity always corresponds to high dissolved oxygen concentration. The highest chlorophyll values existed in the upper layer near the entrance of the estuary in summer (Fig. 5B). The blooms in the middle of the estuary and at depth during the dry season were absent in the wet season. Similar distributions of chlorophyll/phytoplankton in the PRE were also shown in previous studies (Cai et al., 2004; He et al., 2010; Huang et al., 2004; Qiu et al., 2010) where all studies found that in the wet season, the highest chlorophyll was generally in the lower part of the estuary, while in dry season, higher chlorophyll was mainly observed mid-estuary. The spatial and temporal variabilities of the blooms appeared to have close correlation with the seasonal hydrographic characteristics (Fig. 3) that is, in turn, associated with the variable river discharge. They represented the processes jointly controlled by the water residence time, water column stability, and turbidity in the PRE, although details of these processes remain unclear. Quantitative assessment of these concurrent forcing elements on the phytoplankton bloom in the PRE is provided in next section.

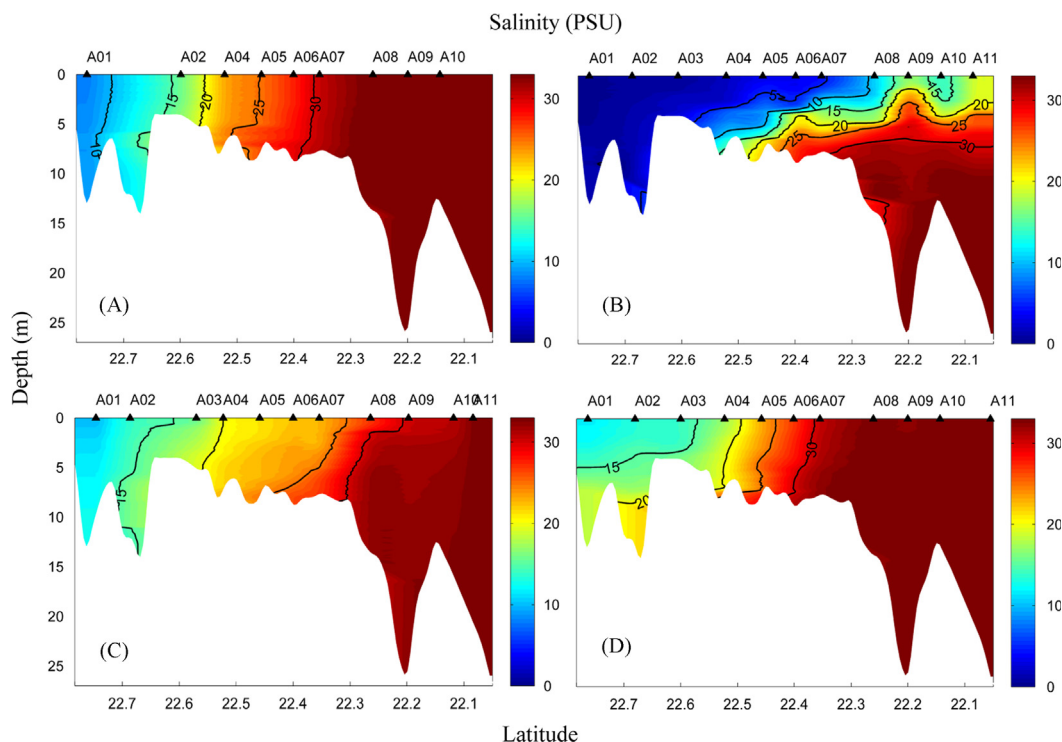


Fig. 3. The vertical distribution of salinity along section A for different seasons in the PRE: (A) April 2010 for spring, (B) August 2010 for summer, (C) November 2010 for autumn, and (D) January 2011 for winter. (For interpretation of the references to color in this figure caption, the reader is referred to the web version of this paper.)

4. Analyses and discussions

As described in the previous section, the location of the phytoplankton bloom was highly variable in different seasons along the PRE. In general, the bloom will occur only when the depth integrated production exceeds the depth integrated loss (Obata et al., 1996; Sverdrup, 1953). In an estuary, factors such as river discharge, wind/tidal mixing, and light availability largely control the residence time, stability, and phytoplankton growth rate in the water column and regulate the temporal and spatial distribution of the bloom (Cloern, 1996).

The PRE is a complex and integrated system where various processes occur and interact with each other concurrently. We will first examine the effect of each individual bloom-controlling factor, and then their joint regulation on the phytoplankton bloom in the PRE.

4.1. Residence time

Residence time of freshwater is defined as $\tau = V/q$, where τ is the residence time, V is the volume of a given pool, and q is the flow rate. Residence time is a very important parameter of the pelagic ecosystem and is associated with the flow field by definition. For a given pool, the increase of phytoplankton biomass from growth will exceed the loss from dilution only when the water residence time is longer than a critical value (Cloern et al., 1983; Malone, 1977; Relexans et al., 1988). This accumulation of phytoplankton biomass is a prerequisite for bloom occurrence.

In an estuary, the residence time varies largely with the seasonal variation of river discharge. By assuming growth is the sole source of phytoplankton biomass increase, and that outflow is the only source of phytoplankton biomass loss, then the change of phytoplankton biomass, P , would be governed by $\partial P/\partial t = \mu P - (q/V)P$, where μ is the growth rate of phytoplankton. Obviously, the bloom would only occur when $\mu > (q/V)$ (Cloern et al., 1985). Here, q/V (the mathematical inverse of τ) is known as

turnover rate (TR), which represents the fraction of water that enters/leaves a given pool in a given time interval. For each cruise in our study, the freshwater flow rate was assumed to be constant. Thus, the residence time gradually increases (turnover rate decreases) from the upper to the lower estuary, as a result of the increase of the total volume in the estuary. Under the regulation of water residence time/turnover rate, the location where $\mu = TR = 1/\tau$ is the critical point for bloom generation along the longitudinal axis of the PRE.

To discuss and evaluate the effect of residence time/turnover rate on the phytoplankton bloom, we created a model in which the PRE was simplified as a trapezoidal prism according to its geographic shape (Fig. 7). The apex represents the entrance of the estuary (Humen outlet, 1 km wide) and the lower side represents the boundary between the PRE and the NSCS (60 km wide). The length of the estuary is ~ 60 km. We used a domain-averaged water depth of 5 m to calculate the volume because the variation of the area of the cross-section along section A is linear (Harrison et al., 2008). We used 10 km as the unit length for the residence time/turnover rate calculation because the blooms in the PRE were generally ~ 10 km in length along the longitudinal axis of the PRE in the spring, autumn, and winter cruises (Fig. 5). Although the total spatial scale of the bloom was > 10 km extending from the lower estuary to the adjacent shelf during the summer cruise, its axial extension inside the PRE was still within ~ 10 km. The variation of water turnover rate in the PRE under different river flow rates is shown in Fig. 8. According to the definition, the turnover rate decreases with the widening of the estuary for a given river discharge rate in a specific season. Meanwhile, at a given location in the PRE, the turnover rate increases with the strengthening of river discharge.

With the exception of nutrient availability and species composition, the growth rate of phytoplankton is mainly regulated by temperature and light availability (Fasham et al., 1990). Therefore, the in situ phytoplankton growth rate in the PRE for each cruise can be estimated from incubation experiments, the relationship

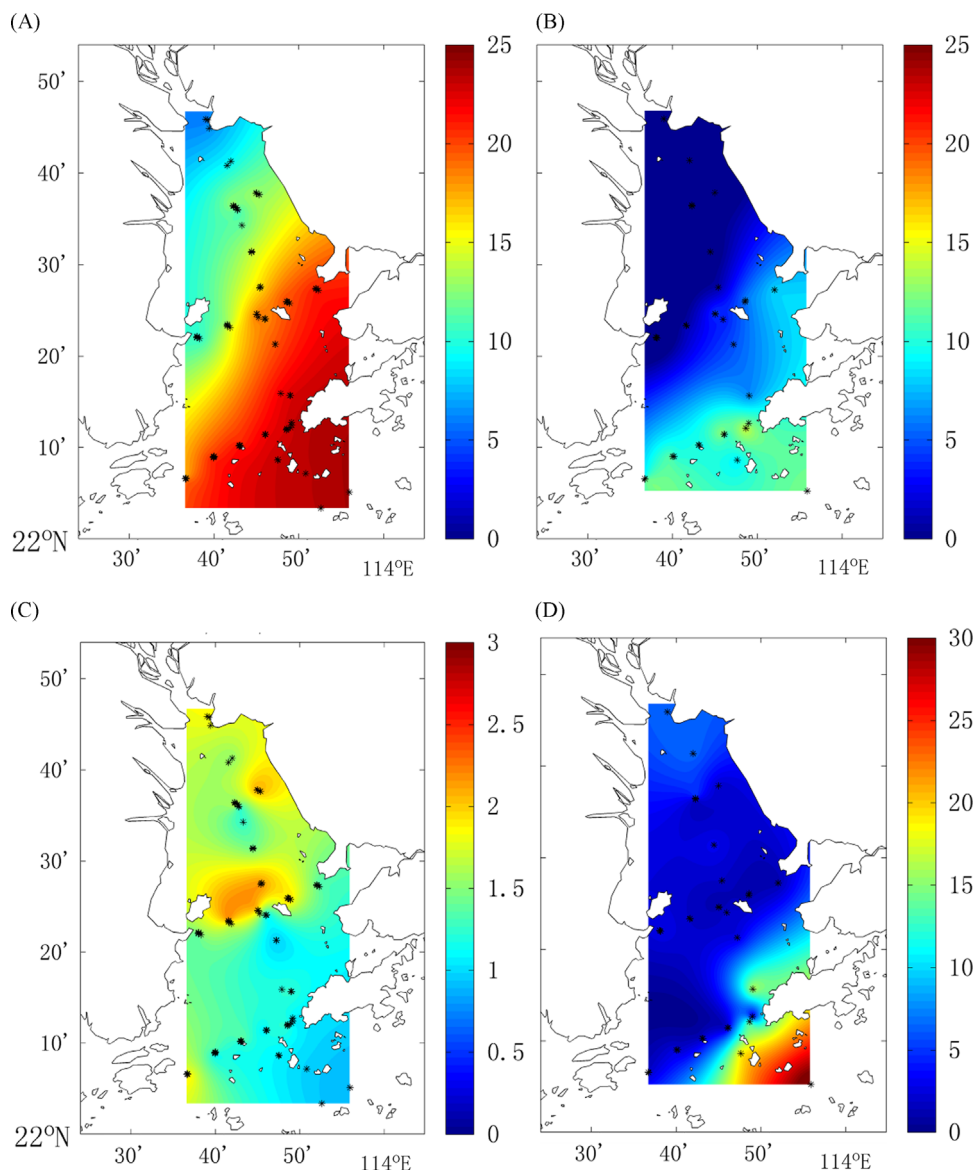


Fig. 4. The horizontal distribution of (A, B) density (kg m^{-3}) and (C, D) chlorophyll ($\mu\text{g L}^{-1}$) in (left column) dry and (right column) wet seasons in the PRE. The density is represented by the density anomaly ($\sigma\text{-t}$, = density – 1000). Dry season was averaged from spring, autumn, and winter; wet season was represented by summer. The data were averaged over the top 5 m of the surface. (For interpretation of the references to color in this figure caption, the reader is referred to the web version of this paper.)

between growth rate and temperature, and the relationship between growth rate and light. Yin et al. (2000) conducted a series of on-deck incubation experiments in the PRE during a cruise in July 1998 and found that the phytoplankton growth rate increased with salinity. As indicated in Figs. 3 and 5, the salinity at the position of the bloom during the dry season varied from 20 to 25. Within this range, the experimental growth rate was 2.36 d^{-1} . Meanwhile, the phytoplankton growth rate is also a function of temperature. The growth rate under different temperatures in spring, autumn, and winter cruises can be estimated with the empirical equation (Eppley, 1972): $\mu_T = \mu_0 \cdot 1.066^T$, where μ_T is the growth rate at temperature T , and μ_0 is the growth rate at 0°C . The water temperatures at the position of the bloom during the spring, autumn, and winter cruises were 21°C , 22°C , and 18°C , respectively. With the incubation temperature of $\sim 28^\circ\text{C}$ (i.e. $\mu_{28} = \mu_0 \cdot 1.066^{28}$), we calculated the phytoplankton growth rates at the position of the bloom during spring, autumn, and winter cruises to be 1.51 d^{-1} , 1.61 d^{-1} and 1.25 d^{-1} , respectively. Similarly, the salinity at the position of the bloom during summer was ~ 15 . The corresponding experimental growth rate was $\sim 1.7 \text{ d}^{-1}$

and the water temperature at the position of the bloom was 28°C . Therefore, we estimated the phytoplankton growth rate during the summer cruise to be $\sim 1.7 \text{ d}^{-1}$.

To evaluate the effect of water residence time/turnover rate on the phytoplankton bloom, the average growth rate in the whole water column should be used. The above estimated phytoplankton growth rate is the potential maximum value under the light immediately below the surface of the water. To obtain the growth rate averaged over the whole water column, we need to consider the effect of light attenuation in the water column. Phytoplankton growth depends on the photosynthesis-light function $f(I) = \alpha I / \sqrt{\mu_T^2 + \alpha^2 I^2}$, in which I represents the light intensity and α represents the initial slope of the $P-I$ curve (0.125 was applied in this case) (Evans and Parslow, 1985). In general, the light in water decreases exponentially with depth or $I_z = I_0 \times \exp(-k \times z)$ (Fennel et al., 2006), where I_z is the light intensity at z meters below the surface, I_0 is light intensity at the sea surface, and k is the light attenuation coefficient. Z_{eu} is the depth of the euphotic layer, through which the light intensity is reduced to 1% of its

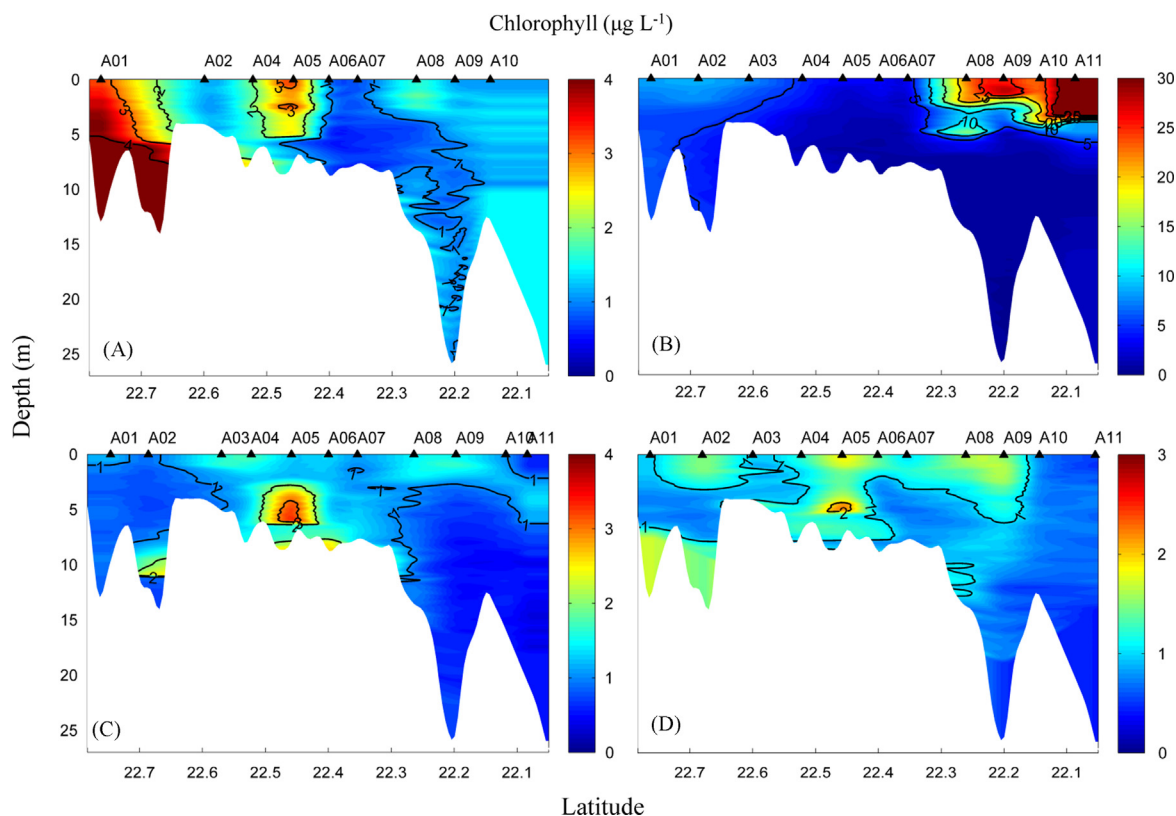


Fig. 5. The vertical distribution of chlorophyll along section A for different seasons in the PRE: (A) April 2010 for spring, (B) August 2010 for summer, (C) November 2010 for autumn, and (D) January 2011 for winter. (For interpretation of the references to color in this figure caption, the reader is referred to the web version of this paper.)

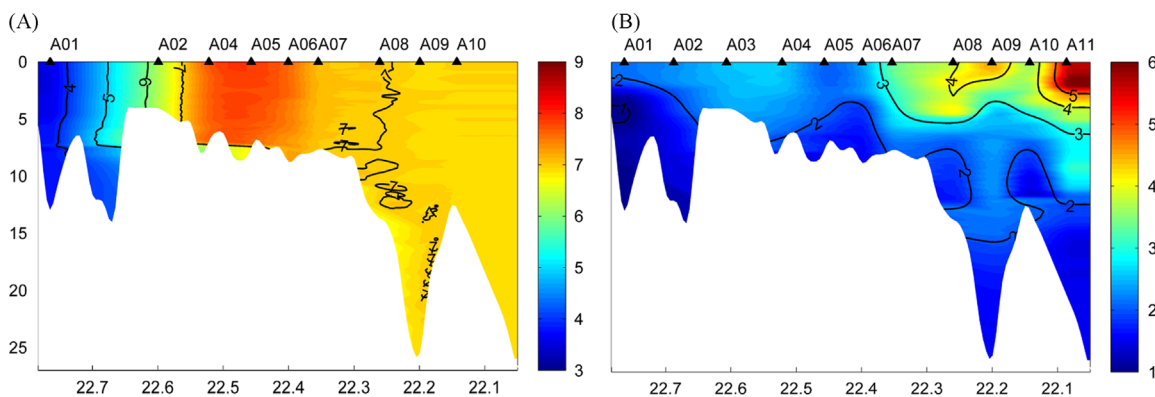


Fig. 6. The vertical distribution of dissolved oxygen (mg L^{-1}) along section A for different seasons in the PRE: (A) April 2010 for spring and (B) August 2010 for summer. The data were obtained from a CTD sensor. (For interpretation of the references to color in this figure caption, the reader is referred to the web version of this paper.)

surface value. It is obtained from Secchi depth (SD) (Preisendorfer, 1986) measurement, $Z_{\text{eu}} = m \times \text{SD}$, where $m \sim 2$ (Aarup, 2002). The Z_{eu} in the PRE along section A varied from ~ 0.7 m upstream to ~ 1.6 m downstream (Fig. 9). Fig. 10 is a schematic diagram showing the vertical profile of I_z and $f(I)$ in the euphotic layer. Values of I_0 for each cruise were derived from the monthly average solar radiation record from the Hong Kong Observatory (http://www.weather.gov.hk/cis/normal/1971_2000/normals_c.htm): 137 W m^{-2} for spring (April), 186 W m^{-2} for summer (August), 146 W m^{-2} for autumn (November), and 122 W m^{-2} for winter (January). According to the Secchi depth measurement, a spatial variable k was adopted in the light intensity calculation of the water column, which was ~ 4.6 mid-estuary and ~ 3.3 in the lower estuary with respective Z_{eu} of ~ 1 m and ~ 1.4 m. By obtaining the growth rate at specific salinity and temperature

using incubation growth rate, Eppley's formulation, and light availability, we derived the depth-dependent growth rate, averaged over the water column, to be 0.19 d^{-1} , 0.34 d^{-1} , 0.21 d^{-1} , and 0.16 d^{-1} for the spring, summer, autumn, and winter, respectively.

Under a given river discharge rate, the location of the residence time/turnover rate critical point for phytoplankton bloom can be estimated from $\mu = TR$. The residence time/turnover rate critical points for each cruise are shown in Fig. 8. Taking the autumn cruise as an example, q was $2553 \text{ m}^3 \text{ s}^{-1}$, μ was estimated to be 0.21 d^{-1} , so the bloom could only be generated when $TR < 0.21$ or where the width of estuary is greater than $\sim 22 \text{ km}$ ($\sim 22.5^\circ \text{N}$). Therefore, if we consider the water residence time/turnover rate as the only regulator, the satisfactory turnover rate for the phytoplankton bloom during the autumn cruise would occur seaward of 22.5°N .

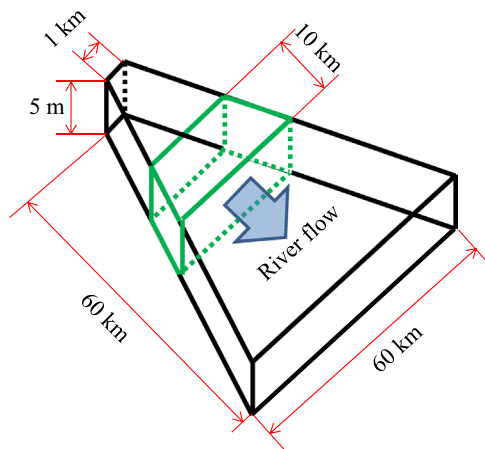


Fig. 7. Sketch of the simplified PRE model. The black trapezoidal prism represents the PRE, and the green trapezoidal prism represents the moving unit for residence time/turnover rate calculation. (For interpretation of the references to color in this figure caption, the reader is referred to the web version of this paper.)

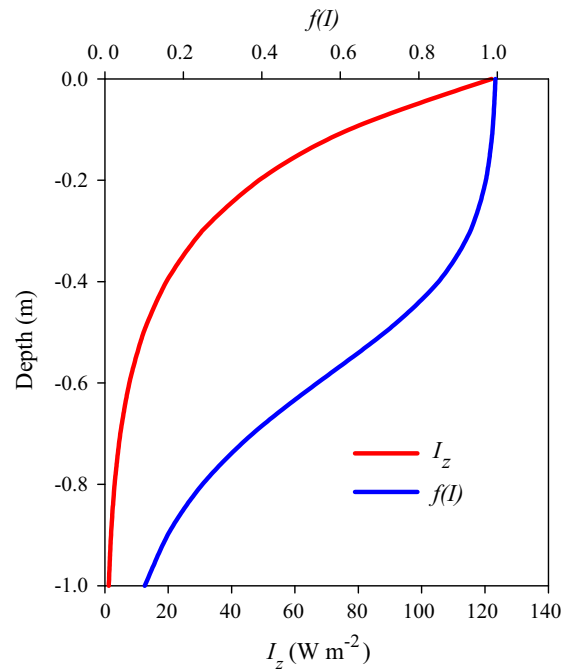


Fig. 10. Schematic diagram of the vertical profile of light intensity (I_z) and photosynthesis-light function ($f(I)$) in the water column. The light intensity immediately below the water surface (I_0) for winter (122 W m^{-2}) was applied for the $f(I)$ calculation. (For interpretation of the references to color in this figure caption, the reader is referred to the web version of this paper.)

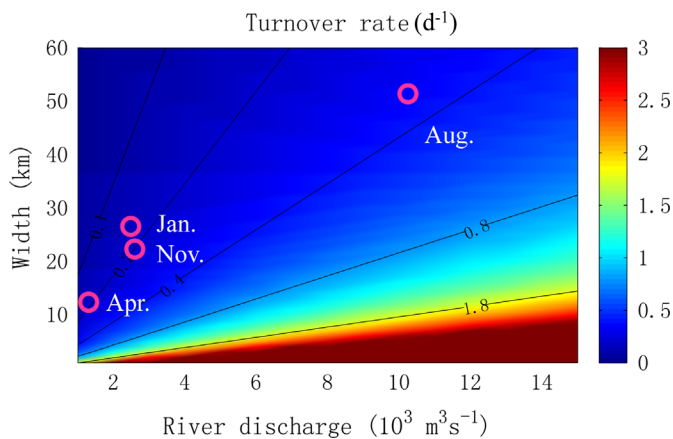


Fig. 8. The water turnover rate as a function of width of the PRE and freshwater discharge of the Pearl River. The pink open circles indicate the locations of critical points for the phytoplankton bloom in different seasons. (For interpretation of the references to color in this figure caption, the reader is referred to the web version of this paper.)

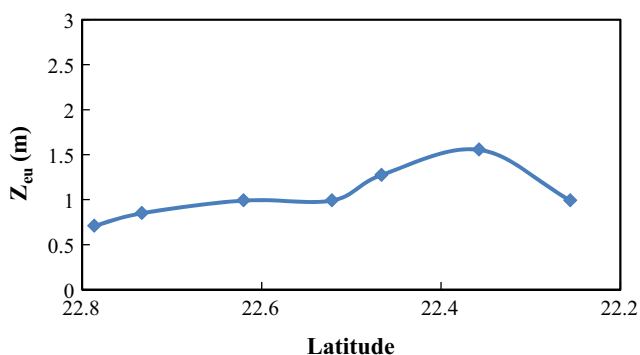


Fig. 9. The depth of the euphotic layer (Z_{eu}) along section A derived from Secchi disk measurements. (For interpretation of the references to color in this figure caption, the reader is referred to the web version of this paper.)

Comparing the results in Fig. 8 with the observations in Fig. 5, we find that the estimated bloom starting points (i.e. the critical points) matched the observed ones quite well during the summer, autumn, and winter cruises, with $\sim 22.5^\circ\text{N}$ for the autumn/winter

cruises and $\sim 22.2^\circ\text{N}$ for the summer cruise. However, the above analysis cannot explain why the observed blooms during the autumn and the winter cruises covered a spatial length scale of only $\sim 10 \text{ km}$ in the region seaward of 22.5°N and why the bloom was absent in the rest of the bloom-favorable region. Moreover, TR as a sole controller of the bloom was totally invalid for the spring cruise. The bloom favorable region during spring should be downstream of $\sim 22.7^\circ\text{N}$ according to Fig. 8, but the observations showed that the bloom started farther downstream at $\sim 22.5^\circ\text{N}$ over a strip of only $\sim 10 \text{ km}$. Clearly, other controlling processes/factors must be considered for the occurrence of the phytoplankton bloom in the PRE.

4.2. Water column stability

It is well-known that water column stability is essential for phytoplankton growth. A bloom will only develop when the mixing depth is less than a critical depth in which the water column integrated production exceeds the water column integrated respiration (Sverdrup, 1953). In the PRE, the buoyancy input by freshwater discharge was the major source of the vertical density gradient. At the same time, turbulence induced by the vertical velocity shear of tidal circulation tended to vertically mix the water and weaken the stratification. Because the euphotic layer of the PRE was quite shallow, the phytoplankton bloom can only be generated when vertical stratification/mixing was strong/weak enough to ensure a net growth within the euphotic layer.

Water column stability can be indicated by the Richardson number $Ri = -g(\partial\rho/\partial z)/\rho((\partial u/\partial z)^2 + (\partial v/\partial z)^2)$, where ρ is potential density, g is the gravitational acceleration, z is the vertical coordinate directed upward, u is the east-west velocity component, and v is the north-south velocity component. Large/small Ri indicates a relatively stable/unstable condition (Miles, 1961). In this study, CTD and ADCP data, sampled from stations A01–A11, along section A, were used to estimate Ri . Fig. 11 shows Ri averaged over the whole water column for different seasons.

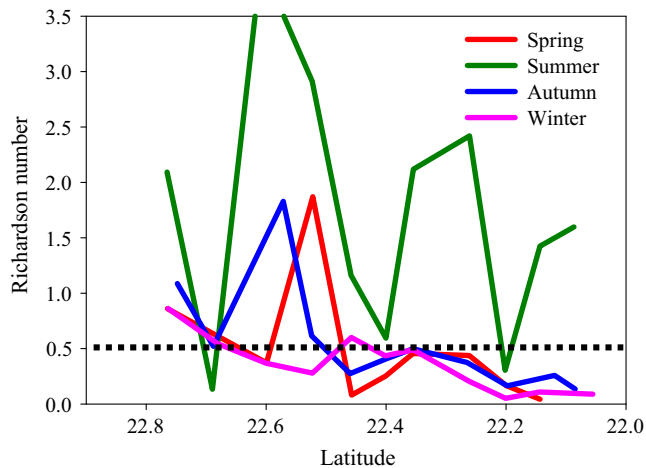


Fig. 11. Depth-averaged Ri along section A for spring, summer, autumn, and winter cruises. The dotted line represents the critical value of Ri . (For interpretation of the references to color in this figure caption, the reader is referred to the web version of this paper.)

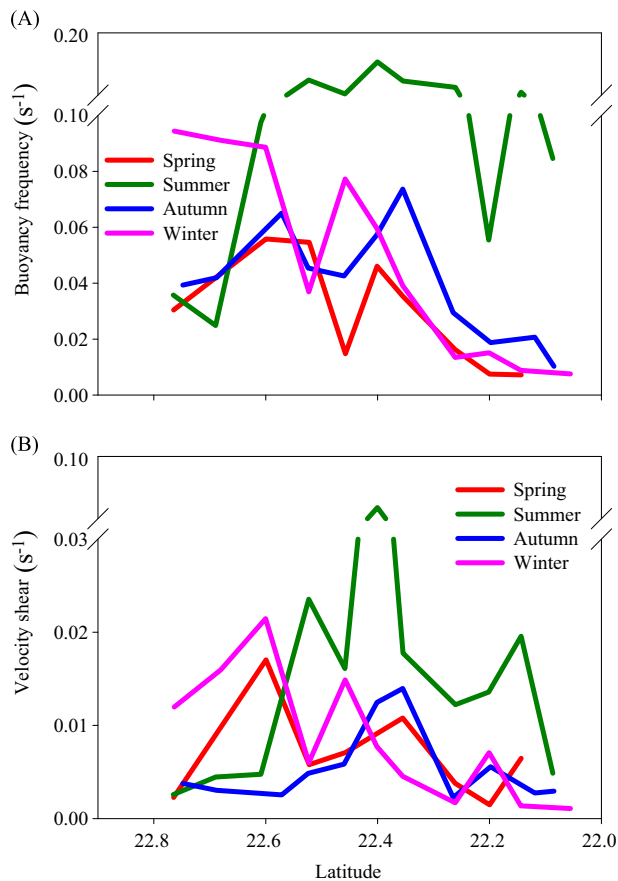


Fig. 12. Depth-averaged (A) buoyancy frequency and (B) vertical velocity shear along section A during spring, summer, autumn, and winter.

Data from the four cruises (Fig. 11) show a common decreasing Ri from upper to lower estuary. According to its definition, Ri is a measure of relative importance of water column stratification to vertical velocity shear. Stratification is indicated by buoyancy frequency: $\sqrt{-(g/\rho)(\partial\rho/\partial z)}$ and shear is defined as $(\partial u/\partial z)^2 + (\partial v/\partial z)^2$. Fig. 12A shows that the stratification of the water column was weakening seaward as freshwater was mainly trapped in the upper part of the PRE during the dry season. During the wet

season, the high river discharge, with freshwater in the upper layer and seawater in the bottom layer, formed a strongly stratified water column in the middle and lower estuary. The patterns of along-estuary variation of the vertical velocity shear (Fig. 12B) were similar to those in the stratification: weak in the nearly barotropic flow in the partially or well-mixed estuary during the dry season, and strong in the two-layer flow in the stratified estuary during the wet season. The combined stability effects of stratification and vertical velocity shear, as reflected in Ri , led to a relatively stable water column upstream where buoyancy input by river discharge dominated and a less stable or unstable water column downstream where vertical velocity shear overcame the weakened stratification.

According to Miles (1961), $Ri > 0.25$ is critical and necessary for the stability of stratified shear flow to occur. However, in general, an experimental range of 0.4–0.8 was often suggested as the approximate critical value (Ellison and Turner, 1959; Price et al., 1978). In this study, the value of $Ri=0.5$ was selected to separate the relatively stable and unstable water columns so that $Ri > 0.5$, averaged over the whole water column, meant that conditions were bloom-favorable. Based on that criterion, we found from Fig. 11 that bloom-favorable conditions only existed in the upper estuary during spring, autumn, and winter, and that the critical position for the transition from static stability to dynamic instability was roughly located at $\sim 22.4^\circ\text{N}$. During these seasons, the phytoplankton bloom occurred upstream of the critical position and was absent downstream of the stability critical position, as seen in the observed chlorophyll distributions (Fig. 5). Among these three cruises, Ri rapidly increased upstream of the critical position for the spring and autumn cruises (Fig. 11). In contrast, Ri remained relatively small over the entire estuary during the winter cruise. As a result, the bloom was generally stronger in spring and autumn and it was relatively weak in winter. Vertical mixing by the strong northeasterly monsoon was likely the reason for the less stable water column in winter. During the summer cruise, $Ri \gg 0.5$ throughout the estuary due to the extremely strong vertical gradient of density (Figs. 3 and 12A).

The combined effect of seasonal variation of residence time and water column stability explains the observed bloom occurrence in summer, autumn, and winter. However, these combined effects still failed to explain why there was no bloom between $\sim 22.5^\circ\text{N}$ and 22.7°N , where the conditions of both residence time/turnover rate and water column stability were all favorable. Another controlling factor must be introduced to provide the answer.

4.3. Turbidity maximum

Light is essential for phytoplankton growth. Light limitation was frequently reported in the PRE because the estuary's turbidity was generally high due to terrestrial input and waste water discharge (Xu, 2007; Yin et al., 2000; Zhang et al., 1999). In general, a turbidity maximum exists in the upper reach of estuaries as the result of sediment resuspension and flocculation (Schubel, 1968), where phytoplankton growth and productivity have the lowest value (Cloern, 1987).

In this study, we used suspended sediment concentration data obtained from seasonal field observations by Wai et al. (2004) and turbidity data from the supplementary cruise along section A in July 2011. The turbidity in the PRE was generally high between $\sim 22.35^\circ\text{N}$ and 22.75°N , with values of turbidity maxima embedded between the two latitudes (Fig. 13). The turbidity maximum in the dry season tended to shift upstream due to low river discharge rate. The turbidity was much higher in the dry season than in the wet season, as seen in the suspended sediment concentration (SSC). During the dry season, the turbidity maximum mostly occurred in the bloom-free region north of $\sim 22.5^\circ\text{N}$

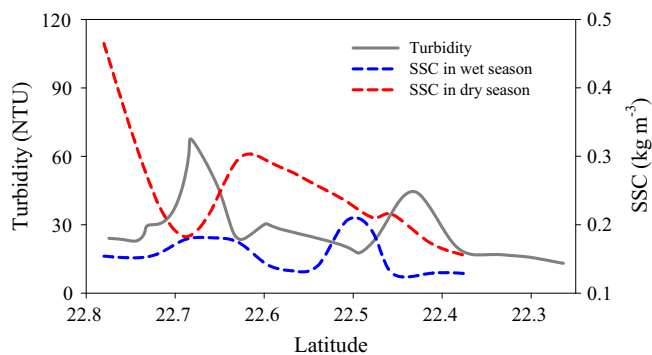


Fig. 13. Surface turbidity (gray solid line) distribution along section A in July 2011 and surface suspended sediment concentration (SSC) distribution digitized from Wai et al. (2004). The blue dashed line and the red dashed line represent the wet and dry season surface SSC, respectively. It is the mathematical mean of the SSC in the West and East channel after being projected to a realistic distance. (For interpretation of the references to color in this figure caption, the reader is referred to the web version of this paper.)

(Fig. 5). This, in particular, offered an explanation for the absence of a bloom between $\sim 22.5^{\circ}\text{N}$ and 22.7°N during spring, even though the conditions of both residence time/turnover rate and water column stability were favorable. A turbidity maximum in the upper reach of the PRE was also reported in other studies (Guo et al., 2008; He et al., 2010; Huang et al., 2003), suggesting that light limitation was the dominant control on the bloom in this region.

4.4. The combined effects of all factors

Different bloom regulators have different controlling mechanisms that lead to various potential bloom distribution patterns. Because it is an integrated system, the resulting bloom that appeared in the PRE must have been regulated by a combination of various processes. Fig. 14 shows the combined effects of water residence time, water column stability, and turbidity on the formation of the phytoplankton bloom in the PRE. The bloom-favorable regions derived from the combined effects matched those shown in the field observations very well (Fig. 5).

Spring was the driest season as indicated by the very low river discharge shown in Fig. 2. The water residence time in the PRE in spring was much longer than in other seasons. Therefore, the satisfactory residence time condition for the phytoplankton bloom generation began to appear downstream of $\sim 22.7^{\circ}\text{N}$. Likewise, a satisfactory water column stability could only exist upstream of $\sim 22.45^{\circ}\text{N}$ because the buoyancy input from the freshwater discharge dominated the stability of water column in the PRE. In addition, increased turbidity upstream of $\sim 22.5^{\circ}\text{N}$ suppressed the phytoplankton growth and bloom development. After synthesizing all these controlling factors, the region where all three factors were theoretically bloom-favorable was between 22.45°N and 22.5°N (indicated by the region with overlapped arrow-bars in Fig. 14A). The result agrees reasonably well with the observations shown in Fig. 5A.

In contrast, in summer, the river discharge was ~ 4 – 10 times higher than in other seasons so that the water column was strongly stratified over the entire estuary due to the huge buoyancy input (Fig. 14B). As a result, water column stability was far from a limiting factor in the PRE. The huge river discharge also led to a very short water residence time in the PRE. According to calculations, the bloom favorable residence time could only be achieved downstream of 22.2°N (Fig. 14B), which explains the observed chlorophyll distribution in Fig. 5B. Turbidity was too low to be a limiting factor of the bloom in this region. Thus, the water residence time became a distinct regulator of the bloom under this circumstance.

During the autumn and winter cruises, river flow rates were almost identical (with $\sim 6\%$ difference). The relatively lower river flow rate during these two seasons resulted in a bloom-favorable residence time located farther upstream. However, since the growth rate of phytoplankton was smaller in winter due to lower temperature, the region with bloom-favorable residence time shifted farther downstream. The distributions of water column stability for these two seasons were also similar except that Ri in winter was generally lower. The areas affected by the large values of turbidity in these two seasons were generally upstream of the region with the bloom-favorable residence time. Considering their joint effect, the bloom-favorable region for both autumn and winter was between $\sim 22.38^{\circ}\text{N}$ and 22.5°N (Fig. 14C, D), which was comparable to observations (Fig. 5C, D). Both water residence time and water column stability controlled the bloom in these two seasons.

5. Summary

Unique seasonal variations of the phytoplankton bloom in the nutrient-rich PRE were studied using field observations and associated quantitative assessments of different controlling factors. The PRE was a typical salt-wedged estuary in summer and a partially/well-mixed estuary in other seasons. The bloom was found in the middle part of the estuary during the dry season, but was pushed seaward to occur in the lower part of the estuary during the wet season. We found that the formation and variability of the seasonal bloom were jointly controlled by the spatial and temporal variability of water residence time, water column stability, and turbidity in the estuary. Unlike previous studies, this study, for the first time, presented evidence of the seasonal variation of the phytoplankton blooms in the PRE and quantitatively consolidated different controlling factors that jointly regulate the variation.

Water residence time in the PRE is highly variable due to the strong seasonal variation of river discharge and acts as an important regulator to the pelagic ecosystem. With fixed river discharge, it increases gradually from the upper estuary towards the lower estuary due to variable geometric conditions. The phytoplankton bloom tends to be generated in the region where the growth rate is greater than the water turnover rate (the mathematical inverse of residence time). The bloom-favorable residence time is a necessary condition for its development. In general, the higher the river discharge, the farther downstream the bloom would start. By synthesizing residence time/turnover rate with the depth-averaged phytoplankton growth rate, the region with bloom-favorable residence time in the PRE was estimated to be in the region downstream of about 22.7 , 22.2 , and 22.5°N for spring, summer, and autumn/winter, respectively. In this study, we utilized the approach that combines the incubation experiments with the growth rate–temperature relation and photosynthesis–light function to derive the average growth rate of phytoplankton in the euphotic layer.

The regulation of water column stability on the phytoplankton bloom was evaluated by examining the Richardson number (Ri) along the longitudinal axis of the PRE, given that a stable water body is favorable for the bloom to occur. Under the interaction of buoyancy input from river discharge and vertical velocity shear induced by estuary circulation, Ri generally decreased from the upper to lower estuary. This indicated a downstream weakening of water column stability and worsening of a bloom generating condition. With seasonal variation of physical forcing associated with the changes in monsoon winds and river discharge, the critical position where static stability turned to dynamic instability was identified to be around 22.4°N in the dry season. However, the water column was dominated by a stable stratification due to the huge river discharge in the wet season and the stability was far from limiting the bloom over the entire estuary.

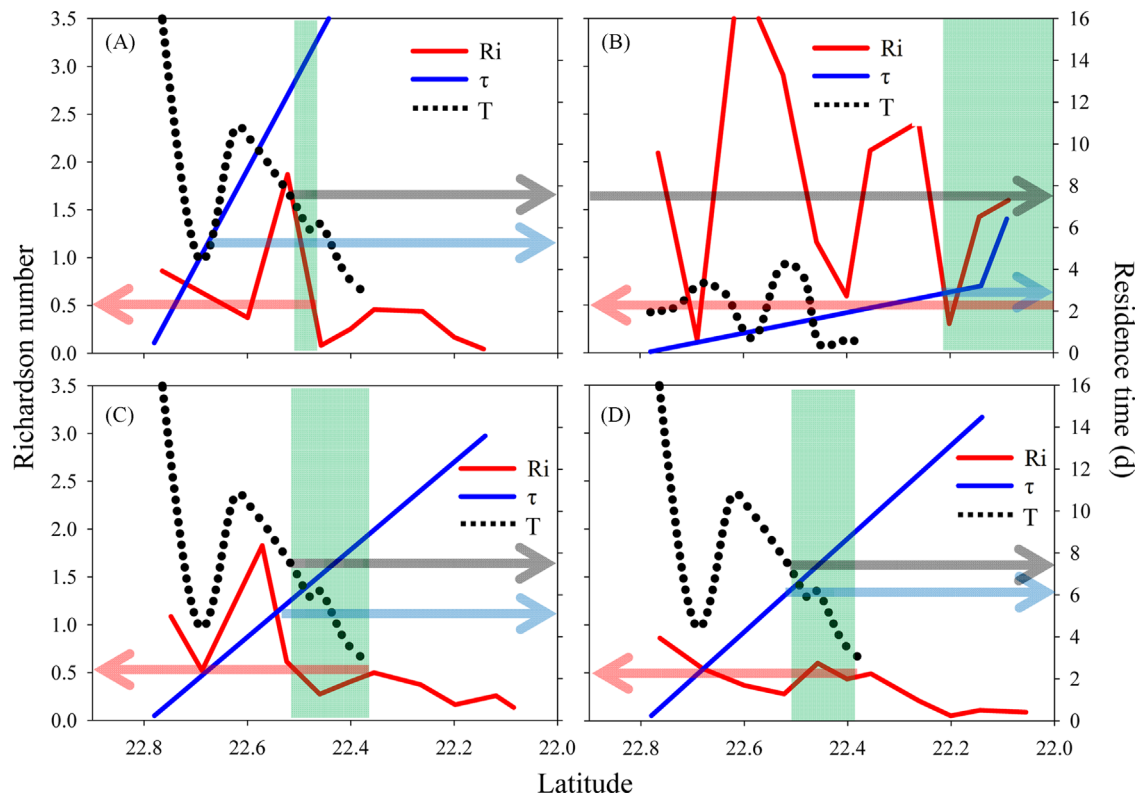


Fig. 14. Combined effects of all bloom controlling factors and calculated bloom occurrence locations along section A for different seasons in the PRE: (A) April 2010 for spring, (B) August 2010 for summer, (C) November 2010 for autumn, and (D) January 2011 for winter. The turbidity (T, black dotted line) is represented by SSC derived from Wai et al. (2004). It is the mathematical mean of the SSC in the West and East channel. The blue, red, and black arrows represent the bloom-favorable region due to water residence time/turnover rate, water column stability (Ri), and turbidity, respectively. The green shaded area indicates the overlap of different bloom favorable regions. (For interpretation of the references to color in this figure caption, the reader is referred to the web version of this paper.)

The increasing turbidity towards the upper reach of the estuary hindered the development of phytoplankton blooms, even when other bloom controlling factors were favorable. When river discharge was very low, it was the turbidity maximum that prevented the formation of the phytoplankton bloom in the upper reach (~22.5–22.8°N) of the PRE.

Although all controlling factors concurrently controlled the blooms, we found that the key controlling factor(s) for the development of the phytoplankton bloom in the PRE was residence time/stability/turbidity, residence time, and residence time/stability in spring, summer, and autumn/winter, respectively.

Acknowledgments

This research was supported by NSFC under project 41276106, by the Centre for Marine Environmental Research and Innovative Technology (MERIT) under projects AOE/P-04/04-5-II and VPRD009/10.SCO4, and by the General Research Fund of the Hong Kong Research Grant Council under projects 612412 and N_HKUST627/13. We thank Xiaozheng Zhao for plotting part of the figures. We also thank Yongqiang Liang and the crew of Yue Dongguang 00589 for their assistance during the cruises. Thoughtful comments and constructive suggestions from three anonymous reviewers are appreciated.

References

Aarup, T., 2002. Transparency of the North Sea and Baltic Sea – a Secchi depth data mining study. *Oceanologia* 44 (3), 323–337.
 Cai, W.J., Dai, M.H., Wang, Y.C., Zhai, W.D., Huang, T., Chen, S.T., Zhang, F., Chen, Z.Z., Wang, Z.H., 2004. The biogeochemistry of inorganic carbon and nutrients in the Pearl River estuary and the adjacent Northern South China Sea. *Cont. Shelf Res.* 24 (12), 1301–1319.

Chen, C.S., Ji, R.B., Schwab, D.J., Beletsky, D., Fahnenstiel, G.L., Jiang, M.S., Johengen, T.H., Vanderploeg, H., Eadie, B., Budd, J.W., Bundy, M.H., Gardner, W., Cotner, J., Lavrentyev, P.J., 2002. A model study of the coupled biological and physical dynamics in Lake Michigan. *Ecol. Model.* 152 (2–3), 145–168.
 Cloern, J.E., Alpine, A.E., Cole, B.E., Wong, R.L.J., Arthur, J.F., Ball, M.D., 1983. River discharge controls phytoplankton dynamics in the northern San-Francisco Bay Estuary. *Estuar. Coast. Shelf Sci.* 16 (4), 415–8.
 Cloern, J.E., Cole, B.E., Wong, R.L.J., Alpine, A.E., 1985. Temporal dynamics of estuarine phytoplankton – a case-study of San-Francisco Bay. *Hydrobiologia* 129 (October), 153–176.
 Cloern, J.E., 1987. Turbidity as a control on phytoplankton biomass and productivity in estuaries. *Cont. Shelf Res.* 7 (11–12), 1367–1381.
 Cloern, J.E., 1991. Tidal stirring and phytoplankton bloom dynamics in an estuary. *J. Mar. Res.* 49 (1), 203–221.
 Cloern, J.E., 1996. Phytoplankton bloom dynamics in coastal ecosystems: a review with some general lessons from sustained investigation of San Francisco Bay, California. *Rev. Geophys.* 34 (2), 127–168.
 Dai, M.H., Wang, L., Guo, X., Zhai, W., Li, Q., He, B., Kao, S.J., 2008. Nitrification and inorganic nitrogen distribution in a large perturbed river/estuarine system: the Pearl River Estuary, China. *Biogeosciences* 5 (5), 1227–1244.
 Ellison, T.H., Turner, J.S., 1959. Turbulent entrainment in stratified flows. *J. Fluid Mech.* 6 (3), 423–448.
 Eppley, R.W., 1972. Temperature and phytoplankton growth in sea. *Fish. Bull.* 70 (4), 1063–1085.
 Evans, G.T., Parslow, J.S., 1985. A model of annual plankton cycles. *Biol. Oceanogr.* 3, 327–347.
 Fasham, M.J.R., Ducklow, H.W., McKelvie, S.M., 1990. A nitrogen-based model of plankton dynamics in the oceanic mixed layer. *J. Mar. Res.* 48, 591–639.
 Fennel, K., Wilkin, J., Levin, J., Moisan, J., O'Reilly, J., Haidvogel, D., 2006. Nitrogen cycling in the middle Atlantic Bight: results from a three-dimensional model and implications for the North Atlantic nitrogen budget. *Glob. Biogeochem. Cycles* 20 (3), GB3007 (doi: 3010.1029/2005GB002456).
 Guillaud, J.F., Andrieux, F., Menesguen, A., 2000. Biogeochemical modelling in the Bay of Seine (France): an improvement by introducing phosphorus in nutrient cycles. *J. Mar. Syst.* 25 (3–4), 369–386.
 Guo, X.H., Cai, W.J., Zhai, W.D., Dai, M.H., Wang, Y.C., Chen, B.S., 2008. Seasonal variations in the inorganic carbon system in the Pearl River (Zhujiang) estuary. *Cont. Shelf Res.* 28 (12), 1424–1434.
 Harrison, P.J., Yin, K.D., Lee, J.H.W., Gan, J.P., Liu, H.B., 2008. Physical-biological coupling in the Pearl River Estuary. *Cont. Shelf Res.* 28 (12), 1405–1415.

- He, B.Y., Dai, M.H., Zhai, W.D., Wang, L.F., Wang, K.J., Chen, J.H., Lin, J.R., Han, A.G., Xu, Y.P., 2010. Distribution, degradation and dynamics of dissolved organic carbon and its major compound classes in the Pearl River estuary, China. *Mar. Chem.* 119 (1–4), 52–64.
- Huang, L.M., Jian, W.J., Song, X.Y., Huang, X.P., Liu, S., Qian, P.Y., Yin, K.D., Wu, M., 2004. Species diversity and distribution for phytoplankton of the Pearl River estuary during rainy and dry seasons. *Mar. Pollut. Bull.* 49 (7–8), 588–596.
- Huang, X.P., Huang, L.M., Yue, W.Z., 2003. The characteristics of nutrients and eutrophication in the Pearl River estuary, South China. *Mar. Pollut. Bull.* 47 (1–6), 30–36.
- Huzzey, L.M., Cloern, J.E., Powell, T.M., 1990. Episodic changes in lateral transport and phytoplankton distribution in south San-Francisco Bay. *Limnol. Oceanogr.* 35 (2), 472–478.
- Koseff, J.R., Holen, J.K., Monismith, S.G., Cloern, J.E., 1993. Coupled effects of vertical mixing and benthic grazing on phytoplankton populations in shallow, turbid estuaries. *J. Mar. Res.* 51 (4), 843–868.
- Liu, H., Yin, B., 2007. Annual cycle of carbon, nitrogen and phosphorus in the Bohai Sea: a model study. *Cont. Shelf Res.* 27 (10–11), 1399–1407.
- Lucas, L.V., Koseff, J.R., Monismith, S.G., Cloern, J.E., Thompson, J.K., 1999. Processes governing phytoplankton blooms in estuaries. II: the role of horizontal transport. *Mar. Ecol. – Prog. Ser.* 187, 17–30.
- Mallin, M.A., Cahoon, L.B., McIver, M.R., Parsons, D.C., Shank, G.C., 1999. Alternation of factors limiting phytoplankton production in the Cape Fear River Estuary. *Estuaries* 22 (4), 825–836.
- Malone, T.C., 1977. Environmental regulation of phytoplankton productivity in lower Hudson Estuary. *Estuar. Coast. Mar. Sci.* 5 (2), 157–171.
- Malone, T.C., Conley, D.J., Fisher, T.R., Glibert, P.M., Harding, L.W., Sellner, K.G., 1996. Scales of nutrient-limited phytoplankton productivity in Chesapeake Bay. *Estuaries* 19 (2B), 371–385.
- Masson, D., Pena, A., 2009. Chlorophyll distribution in a temperate estuary: the Strait of Georgia and Juan de Fuca Strait. *Estuar. Coast. Shelf Sci.* 82 (1), 19–28.
- Miles, J.W., 1961. On the stability of heterogeneous shear flows. *J. Fluid Mech.* 10 (4), 496–508.
- Monbet, Y., 1992. Control of phytoplankton biomass in estuaries – a comparative analysis of microtidal and macrotidal estuaries. *Estuaries* 15 (4), 563–571.
- Myers, V.B., Iverson, R.L., 1981. Phosphorus and nitrogen limited phytoplankton productivity in northeastern Gulf of Mexico coastal estuaries. In: Neilson, B.J., Cronin, L.E. (Eds.), *Estuaries and Nutrients*. Humana Press, Clifton, NJ, pp. 569–582.
- O'Boyle, S., Silke, J., 2010. A review of phytoplankton ecology in estuarine and coastal waters around Ireland. *J. Plankton Res.* 32 (1), 99–118.
- Obata, A., Ishizaka, J., Endoh, M., 1996. Global verification of critical depth theory for phytoplankton bloom with climatological in situ temperature and satellite ocean color data. *J. Geophys. Res. – Oceans* 101 (C9), 20657–20667.
- Parekh, P., Follows, M.J., Boyle, E.A., 2005. Decoupling of iron and phosphate in the global ocean. *Glob. Biogeochem. Cycles* 19 (2), GB2020 (doi: 2010.1029/2004GB002280).
- Pennock, J.R., Sharp, J.H., 1994. Temporal alternation between light-limitation and nutrient-limitation of phytoplankton production in a coastal-plain estuary. *Mar. Ecol. – Prog. Ser.* 111 (3), 275–288.
- Preisendorfer, R.W., 1986. Secchi disk science – visual optics of natural-waters. *Limnol. Oceanogr.* 31 (5), 909–926.
- Price, J.F., Mooers, C.N.K., Vanleer, J.C., 1978. Observation and simulation of storm-induced mixed-layer deepening. *J. Phys. Oceanogr.* 8 (4), 582–599.
- Pritchard, D.W., 1967. What is an estuary: physical viewpoint. In: Lauf, G.H. (Ed.), *Estuaries*. American Association for the Advancement of Science, Washington D.C, pp. 3–5.
- Qiu, D.J., Huang, L.M., Zhang, J.L., Lin, S.J., 2010. Phytoplankton dynamics in and near the highly eutrophic Pearl River Estuary, South China Sea. *Cont. Shelf Res.* 30 (2), 177–186.
- Relexans, J.C., Meybeck, M., Billen, G., Brugeaille, M., Etcheber, H., Somville, M., 1988. Algal and microbial processes involved in particulate organic-matter dynamics in the Loire Estuary. *Estuar. Coast. Shelf Sci.* 27 (6), 625–644.
- Schubel, J.R., 1968. Turbidity maximum of northern Chesapeake Bay. *Science* 161 (3845), 1013–1015.
- Sverdrup, H.U., 1953. On conditions for the vernal blooming of phytoplankton. *J. Cons. Cons. Int. l'Exploration Mer* 18 (3), 287–295.
- Tan, Y.H., Huang, L.M., Chen, Q.C., Huang, X.P., 2004. Seasonal variation in zooplankton composition and grazing impact on phytoplankton standing stock in the Pearl River Estuary, China. *Cont. Shelf Res.* 24 (16), 1949–1968.
- Tremblay, J.E., Legendre, L., Therriault, J.C., 1997. Size-differential effects of vertical stability on the biomass and production of phytoplankton in a large estuarine system. *Estuar. Coast. Shelf Sci.* 45 (4), 415–431.
- Twomey, L., Thompson, P., 2001. Nutrient limitation of phytoplankton in a seasonally open bar-built estuary: Wilson inlet, Western Australia. *J. Phycol.* 37 (1), 16–29.
- Wai, O.W.H., Wang, C.H., Li, Y.S., Li, X.D., 2004. The formation mechanisms of phytoplankton turbidity maximum in the Pearl River estuary, China. *Mar. Pollut. Bull.* 48 (5–6), 441–448.
- Xu, J., 2007. Nutrient Limitation in the Pearl River Estuary, Hong Kong Waters and Adjacent South China Sea waters (Ph.D. thesis), Hong Kong University of Science and Technology, Hong Kong, 212 pp.
- Yin, K.D., Qian, P.Y., Chen, J.C., Hsieh, D.P.H., Harrison, P.J., 2000. Dynamics of nutrients and phytoplankton biomass in the Pearl River estuary and adjacent waters of Hong Kong during summer: preliminary evidence for phosphorus and silicon limitation. *Mar. Ecol. – Prog. Ser.* 194, 295–305.
- Yin, K.D., Lin, Z.F., Ke, Z.Y., 2004. Temporal and spatial distribution of dissolved oxygen in the Pearl River Estuary and adjacent coastal waters. *Cont. Shelf Res.* 24 (16), 1935–1948.
- Yin, K.D., Harrison, P.J., 2007. Influence of the Pearl River estuary and vertical mixing in Victoria Harbor on water quality in relation to eutrophication impacts in Hong Kong waters. *Mar. Pollut. Bull.* 54 (6), 646–656.
- Zhai, W., Dai, M., Cai, W.-J., Wang, Y., Wang, Z., 2005. High partial pressure of CO₂ and its maintaining mechanism in a subtropical estuary: the Pearl River estuary, China. *Mar. Chem.* 93, 21–32.
- Zhang, J., Yu, Z.G., Wang, J.T., Ren, J.L., Chen, H.T., Xiong, H., Dong, L.X., Xu, W.Y., 1999. The subtropical Zhujiang (Pearl River) Estuary: nutrient, trace species and their relationship to photosynthesis. *Estuar. Coast. Shelf Sci.* 49 (3), 385–400.
- Zu, T., 2009. Tidal Dynamics in the South China Sea and Estuarine & Adjacent Shelf Circulation in the Pearl River Estuary: Modeling Studies (Ph.D. thesis), Hong Kong University of Science and Technology, Hong Kong.
- Zu, T., Gan, J., 2013. A numerical study of coupled estuary-shelf circulation around the Pearl River Estuary during summer: responses to variable winds, tides and river discharge. *Deep-Sea Res. II*, <http://dx.doi.org/10.1016/j.dsr2.2013.12.010>, this issue.